Carbohydrate Polymers 95 (2013) 404–413

Contents lists available at SciVerse ScienceDirect

Carbohydrate Polymers

journal homepage: www.elsevier.com/locate/carbpol

Carbohydrate plasma expanders for passive tumor targeting: *In vitro and in vivo* studies

Stefan Hoffmann[a], Henrike Caysa[a,b], Judith Kuntsche[c], Patrick Kreideweiß[d], Anja Leimert[e], Thomas Mueller[b], Karsten Mäder[a,*]

[a] Institute of Pharmacy, Pharmaceutical Technology and Biopharmacy, Martin-Luther-University Halle-Wittenberg, 06120 Halle, Germany
[b] Department of Internal Medicine IV, Oncology/Hematology, Martin-Luther-University Halle-Wittenberg, 06120 Halle, Germany
[c] Department of Physics, Chemistry and Pharmacy, University of Southern Denmark, 5230 Odense, Denmark
[d] Institute of Pharmacy, Biochemical Pharmacy, Martin-Luther-University Halle-Wittenberg, 06120 Halle, Germany
[e] Department of Anaesthesiology and Intensive Care Medicine, Martin-Luther-University Halle-Wittenberg, 06120 Halle, Germany

ARTICLE INFO

Article history:
Received 19 December 2012
Received in revised form 1 March 2013
Accepted 7 March 2013
Available online 15 March 2013

Keywords:
Hydroxyethyl starch
HES
Multispectral optical imaging
Tumor accumulation
Passive tumor targeting
Cytokine induction

ABSTRACT

The objective of this study was to investigate the suitability of carbohydrate plasma volume expanders as a novel polymer platform for tumor targeting. Many synthetic polymers have already been synthesized for targeted tumor therapy, but potential advantages of these carbohydrates include inexpensive synthesis, constant availability, a good safety profile, biodegradability and the long clinical use as plasma expanders. Three polymers have been tested for cytotoxicity and cytokine activation in cell cultures and conjugated with a near-infrared fluorescent dye: hydroxyethyl starches (HES 200 kDa and HES 450 kDa) and dextran (DEX 500 kDa). Particle size and molecular weight distribution were determined by asymmetric flow field-flow fractionation (AF4). The biodistribution was investigated non-invasively in nude mice using multispectral optical imaging. The most promising polymer conjugate was characterized in human colon carcinoma xenograft bearing nude mice. A tumor specific accumulation of HES 450 was observed, which proves it's potential as carrier for passive tumor targeting.

1. Introduction

Synthetic polymers have been investigated as drug carriers for the delivery of active compounds for years (Haag & Kratz, 2006; Ulbrich et al., 2000; Vicent, Ringsdorf, & Duncan, 2009). The most considerable advantages of polymer–drug conjugates compared to the free drug are reduced side effects, higher solubility and bioavailability, as well as improved biodistribution and stability (Garnett, 2001). The controlled delivery of anti-tumor agents has especially attracted attention in the field of polymer therapeutics (Duncan, 2009; Kopecek & Kopeckova, 2010; Lammers & Ulbrich, 2010; Maeda, 2001). Copolymers based on N-(2-hydroxypropyl)methacrylamide (HPMA), as water soluble and non-particulate synthetic polymer carriers, have been particularly intensively investigated for the controlled delivery of covalently bound cytotoxic drugs to tumor tissue, but other polymers have been also considered (Bae & Kataoka, 2009; Gillies & Frechet, 2005). It has been shown that high-molecular-weight polymers can lead to passive accumulation in the tumor tissue due to the enhanced permeability and retention (EPR) effect (Maeda & Matsumura, 2011; Matsumura & Maeda, 1986). Although several polymers have been synthesized for this purpose in the last decades and promising results have been obtained in preclinical animal studies, only few entered clinical trials and even less resulted in approved market products (Vicent et al., 2009; Duncan, Ringsdorf, & Satchi-Fainaro, 2006). Disadvantages of new synthetic polymers are often complex synthesis conditions that are difficult to control, resulting in usually only small amounts of products and high costs. Even more important is that the polymers often do not have regulatory status. Therefore extensive toxicity and biocompatibility studies are necessary to proceed from the preclinical to the clinical phase of drug development. Polymers from natural sources are often less expensive and available in a large scale. In the last years, several carbohydrates have attracted attention as building blocks for nanoparticles (Mizrahy & Peer, 2012). In addition, the potential of some carbohydrate drug conjugates has been already demonstrated for polysaccharides of lower molecular weight (Goodarzi, Varshochian, Kamalinia, Atyabi, & Dinarvand, 2012). As a high-molecular-weight carbohydrate for tumor therapy, hyaluronic acid (HA) has been intensively investigated in the last years and some HA–drug conjugates have entered already clinical trials. HA-Irinotecan (Alchemia), for instance, is currently investigated in Phase III for the treatment

* Corresponding author. Tel.: +49 345 55 25 167; fax: +49 345 55 27 029.
E-mail address: karsten.maeder@pharmazie.uni-halle.de (K. Mäder).

0144-8617/$ – see front matter © 2013 Elsevier Ltd. All rights reserved.
http://dx.doi.org/10.1016/j.carbpol.2013.03.033

of colorectal cancer. Plasma volume expanders based on glucose monomers, like hydroxyethyl starch (HES) and dextran (DEX), are known to be well tolerated and biocompatible. High doses of these materials have been used in the clinic for decades (Bowman, 1953; Lee, Cooper, Weidner, & Murner, 1968) and there are several approved products on the market, for instance HyperHES® (Fresenius Kabi), Venofundin® (B. Braun) and Vitafusal® (Serumwerk Bernburg). The production of these polymers is well established and possible in large scales under GMP conditions. Furthermore, HES is presently used to develop new drug delivery systems for parenteral application (Wöhl-Bruhn, Badar, et al., 2012; Wöhl-Bruhn, Bertz, et al., 2012), for gene delivery (Noga et al., 2012), and it also attracted attention as commercial technology (HESylation®) to improve the solubility and to prolong the circulation time of certain active compounds (Hey, Knoller, & Vorstheim, 2011). In our study, three commercially available glucose-based polymers have been investigated with respect to the influence of their molecular weight distribution on the biodistribution and on the long term *in vivo* fate: hydroxyethyl starch 200 kDa (HES 200) and 450 kDa (HES 450) and Dextran 500 kDa (DEX 500). We are aware of the safety issues of high-molecular-weight hydroxyethyl starches in certain severe diseased patients that have been recently discussed (Perner et al., 2012; Navickis, Haynes, & Wilkes, 2012). However the difference in using HES as plasma volume expander (infusion of comparatively large volumes) or in tumor therapy needs to be taken into account. Nevertheless, cytotoxicity and immunogenicity of the carbohydrates evaluated in this study were characterized in hepatocellular carcinoma cells (HepG2) and in human peripheral blood mononuclear cells (PBMC's). For *in vivo* visualization, the polymers were covalently conjugated with a near-infrared (NIR) fluorescent dye (IR800CW) after amine-modification, which influenced their molecular weight distribution. The *in vivo* fate was investigated in nude mice by non-invasive multispectral optical imaging over several weeks and by *ex vivo* imaging of autopsied organs. Recently, the powerful possibilities to characterize the *in vivo* fate of polymers using multispectral optical imaging have been demonstrated for HPMA copolymers and other nanoscaled drug delivery systems (Hoffmann et al., 2012; Schädlich et al., 2012). Advantages of optical imaging are the overall simple setup (*e.g.* no radioactive labels are necessary) and the possibility of long-term observation for up to several months. The use of a NIR fluorescent dye provides high sensitivity and detection of fluorescent signals also in deep tissues like liver and spleen, due to comparatively low tissue absorbance of light in this spectral range (Leblond, Davis, Valdes, & Pogue, 2010). In our study, elimination and biodistribution of the three carbohydrate polymer carriers was characterized *in vivo* over several weeks by use of multispectral fluorescence imaging. Furthermore, the potential of the most promising polymer for passive tumor targeting was confirmed *in vivo* in human xenograft colon carcinomas.

2. Material and methods

2.1. Materials

The polysaccharide polymers HES 200/0.5 (batch 0473), HES 450/0.7 (batch 00209) and dextran 500 (batch 241/03) were kindly provided by Serumwerk Bernburg AG, Germany. The near-infrared fluorescent dye IR800CW was purchased from LI-COR, US. Ethylene diamine, p-toluenesulfonyl chloride and deuterium oxide, lipopolysaccharide (LPS) from *Escherichia coli* 055:B5 and cell culture supplements were obtained from Sigma–Aldrich, Germany. Lymphocyte separation medium (LSM 1077), sodium pyruvate solution and MEM cell culture medium containing phenol red were from PAA Laboratories, Austria. Gibco® MEM without phenol red was purchased from Life Technologies, USA. HepG2 cells were purchased from the Leibnitz Institute DSMZ-German Collection of Microorganisms and Cell Cultures, Germany. BD CBA human inflammatory cytokines kit was bought from Becton, Dickinson and Company, USA. Dimethylformamide (DMF) and triethylamine were HPLC grade and used as received from VWR, Germany. Water was bi-distilled before use. The dialysis membrane (MWCO 3.5 kDa) for product purification was purchased from Spectrum Labs, USA. Sterile filters (0.2 μm) were obtained from Millipore, USA. Isoflurane (Forane®) was purchased from Abbott, Germany. All other chemicals and materials were used as received.

2.2. In vitro toxicity in HepG2 cells

The cytotoxicity of the polysaccharide solutions was investigated by the MTT assay. The polymers were dissolved in phosphate buffered saline (PBS) at stock concentrations of 200 mg/mL and 20 mg/mL. The solutions were diluted 1:10 (v/v) with MEM medium with Earl's salt and phenol red (supplemented with 10% FBS, sodium pyruvate solution, non-essential amino acid solution and gentamicin–glutamine solution). HepG2 cells (3×10^4 cells/well) were grown at 37 °C and 5% CO_2 atmosphere in a 96-well plate in the same supplemented MEM medium with Earl's salt and phenol red. After 24 h, the medium was removed and 100 μL polymer solution were added to each well. After incubation for 24 h or 48 h, the supernatant was removed and cells were incubated with 100 μL solution of MTT (500 μg/mL) in indicator-free MEM medium without supplements for 3 h. Cells were lysed subsequently with 100 μL lysis buffer (5 g sodium dodecylsulfate, 0.3 mL acetic acid and 49.7 mL DMSO) for 1 h and absorption was measured with a microplate reader (BMG Labtech Polarstar Omega) at 570 nm. Non-treated cells were used as a reference (positive control) and cells treated with 100 μL DMSO (30%, v/v in MEM) were the negative control.

2.3. In vitro cytokine induction assay

Stimulation of inflammatory cytokines was investigated in human peripheral blood monocyte cells (PBMC's). Heparinized blood was obtained from 3 healthy donors and PBMC's were isolated by density gradient centrifugation ($2000 \times g$, Heraeus Biofuge Stratos) on lymphocyte separation medium (LSM 1077). After washing with PBS, cells were resuspended in RPMI 1640 medium containing 10% inactivated human serum from the same donor and seeded in a 24-well plate at a concentration of 5×10^5 cells per well. 10 μL of polymer solution (200 mg/mL in PBS) were added to the sample wells. 20 μL solution of lipopolysaccharide from *E. coli* (LPS, 1 μg/mL) were used as positive control and 10 μL PBS as negative control. RPMI 1640 medium containing 10% inactivated human serum was added to the wells to give a total volume of 1 mL per well and the cells were incubated at 37 °C and 5% CO_2 atmosphere. After incubation for 4 h or 24 h, supernatants were aspirated, centrifuged 3 min at $18{,}500 \times g$ (Hettich Mikro 200R) and immediately frozen in liquid nitrogen. Cell viability was checked after 4 h and 24 h by Trypan blue exclusion and always found to be >95%. Inflammatory cytokines (IL-1β, IL-6, IL-8, IL-10, IL-12p70 and TNF) were analyzed by a cytometric multibead assay using the BD CBA human inflammatory cytokines kit and following the kit instructions. A 10-point calibration curve was measured between 20 pg/mL and 5000 pg/mL. Measurements of the beads were performed on a BD LSR II Fortessa™ Cell Analyzer on FL2 and FL3 channel using the FACS Diva™ Software and the results were analyzed using FCAP Array™ Software (Version 3.0). All measurements were performed in independent duplicates and the results are given as a mean of duplicate measurements from 3 different blood samples.

2.4. Synthesis of stable polymer–dye conjugates

Amine functions were introduced to all three polymers prior to conjugation with the dye IR800CW to provide a stable amide bond. For this purpose all polymers were activated with p-toluenesulfonyl chloride based on a previously described method (Besheer, Hertel, Kressler, Mäder, & Pietzsch, 2009). 1 g of HES 200 and HES 450 were each dissolved in 20 mL DMF. 1 g of Dextran 500 was dissolved in 20 mL borax buffer (pH 10) as the reaction in DMF did not work here. Tosyl-activation in aqueous media was already previously described (Morita, Nakatsuji, Misaki, & Tanabe, 2005). All solutions were cooled to 2–4 °C and 2 mL triethylamine were added. 0.3 g (HES 200 and 450) and 0.2 g (DEX 500) toluenesulfonyl chloride were dissolved in 2 mL DMF in the dark and dropwisely added to each polymer solution, which was then stirred for 2 h in the dark at 2–4 °C. The polymers were precipitated by pouring the solutions into 100 mL cold acetone (4 °C), washed 3 times with each 20 mL cold acetone, dried, dissolved in 30 mL water and dialysed against 1.5 L water for 72 h (3.5 kDa membrane, medium was changed 5 times). The resulting solutions were lyophilized afterwards and the reaction success was evaluated by ^{1}H-NMR. 300 mg of the tosyl-activated polymers were dissolved in 50 mL of a mixture of borax buffer (pH 9.5) and DMF (2:1 v/v). 1.5 g of ethylene diamine (500 fold molar excess) were added and the solution was stirred for 2 days at 40 °C (HES 200 and HES 450) or for 1 day at 70 °C (DEX 500) in the dark. The amine-modified polymers were precipitated in a mixture of methanol and 2-propanol (1:1, v/v; 200 mL), washed 3 times with 20 mL methanol/2-propanol, dried, dissolved in 30 mL water, dialysed against water for 72 h as described above and lyophilized. 100 mg of the amine-modified polymers were dissolved in bi-distilled water (50 mL) and reacted with 0.6 mg dye IR800CW-NHS ester in the dark for 2 h at 4 °C and a pH of 8.5 and subsequently dialysed against water and lyophilized afterwards. Unmodified dextran 500 (60 mg) was conjugated with 0.4 mg IR800CW-NHS ester to serve as an ester control using the same reaction parameters. The polymer solution was frozen in liquid nitrogen immediately after the reaction and subsequently lyophilized to avoid ester hydrolysis.

2.5. Nuclear magnetic resonance spectroscopy

Success of the activation and of the cleavage of the tosyl functions was proven by ^{1}H-NMR. 7 mg of polymer were dissolved in 700 μL D_2O and ^{1}H-NMR spectra were recorded at 400 MHz using a Gemini 2000 spectrometer (Varian Inc.).

2.6. Particle size and molecular weight distribution

Particle size distributions of all polymers were measured by dynamic light scattering (DLS, Zetasizer nano, Malvern). Samples were dissolved in bi-distilled water (10 mg/mL) and filtered (0.45 μm) prior to measurement at 25 °C ($n = 4$). To confirm the results and to determine the molecular weight distribution, asymmetric flow field-flow fractionation (AF4, Eclipse) combined with a multi-angle light scattering detector (MALLS, DAWN EOS) and an RI detector (Shodex 101) was applied (channel length: 265 mm, height 350 μm, membrane: polyethersulfone MWCO 5k from Wyatt (Germany), carrier liquid: PBS preserved with 0.02% sodium azide and filtered through 0.1 μm). 100 μL of polymer solution (1 mg/mL) in PBS were injected over 2 min (focus flow 2 mL/min) and then eluted with a constant detector flow (1 mL/min) and decreasing cross flow (2 mL/min to 0.1 mL/min in 20 min and 0.1 mL/min to 0 mL/min in 20 min). The molecular weight distributions of the polymers were calculated with the ASTRA software (version 4.90, Wyatt, Germany) based on the light scattering and the RI signals (RI signals were baseline corrected), using the Debye fit method (5th order polynomial). The incremental change of the refractive index (dn/dc), which is needed to calculate the concentration at each elution time and thus the molecular weight, was determined in PBS at 25 °C by injection of different concentrations in the range of 0.2 mg/mL to 1 mg/mL to the RI detector. It was calculated to be 0.142 mL/g (HES 200), 0.146 (HES 450) and 0.145 mL/g (DEX 500), which is in very good agreement with literature data (Kulicke, Kaiser, Schwengers, & Lemmes, 1991). The polymer sizes were calculated as z-average mean square diameters (D_Z) and the molecular weights were calculated as weight averaged molar mass (M_W). All measurements were carried out in triplicate and results are given as average.

2.7. Dye loading

The efficiency of the conjugation with the fluorescent dye was quantified using the Maestro® Fluorescence Imager (Cambridge Research and Instrumentation, USA). Calibration of the emitted fluorescence intensity was carried out with free dye in a concentration range between 0.1 and 0.6 μg/mL in water. 3 mg of conjugated polymer were dissolved in 1 mL bi-distilled water and diluted with bi-distilled water 1:40 (v/v) resulting in a polymer concentration of 75 μg/mL. Fluorescence intensity was measured and the dye content was calculated based on the calibration curve.

2.8. In vivo fluorescence imaging in healthy mice

Biodistribution and elimination of the polymers was investigated over several months in nude female mice (SKH1-Hr^{hr} from Charles River Lab, 3–5 months old at the beginning). All mice were kept under controlled conditions (12 h day/night cycle, 24 °C). The mice were anesthetised with 1.5–2.5% isoflurane (Forane®, Abbott) in oxygen at a flow of 2 L/min for the imaging process. Fluorescence imaging was carried out with the Maestro® Fluorescence Imager (Cambridge Research and Instrumentation, US) using a 710–760 nm excitation filter and a 800 nm long-pass emission filter. During the imaging process, mice were placed on a tempered plate (35 °C) and the isoflurane concentration was adjusted individually. All images were automatically exposed to avoid overexposure and the maestro software (version: 2.10.0) was used to deconvolute the spectral component of the infrared fluorescent dye based on previously recorded spectra of the polymers in bi-distilled water. A total of 15 mg of each polymer was dissolved in 1 mL isotonic sorbitol solution. The solution was sterile-filtered (0.2 μm Millex, Millipore, US) and 100 μL were injected into the tail vein of each mouse ($n = 4$, according 1.5 mg polymer per mouse). A mouse of each group was sacrificed and autopsied one day after injection of the polymer solution to obtain a detailed view on the organ distribution of the polymers. All experiments complied with regional standards and regulations and were approved by the local authority in Saxony-Anhalt.

2.9. In vivo fluorescence imaging in tumor bearing mice

Tumor accumulation of HES 450 was observed in 3 male athymic nude mice (Hsd1Cpb:NMRI-Foxn1, 5 weeks old, from Harlan Winkelmann). After two weeks of setting in period, human colon carcinoma cells were injected to the left (HT-29, 5×10^6 cells) and right (DLD-1, 5×10^6 cells) flank of the mice. Mouse weight and tumor size was continuously measured and the tumor volume was estimated by measurement of tumor length (l) and width (w) (Euhus, Hudd, Laregina, & Johnson, 1986; Tomayko & Reynolds, 1989). The volume was calculated using the equation:

$$V = l \times w^2 \times \frac{\pi}{6}$$

NIR-HES 450 (1.5 mg in 100 μL) in isotonic sorbitol solution was injected into the tail vein of the mice 21 days after tumor cell inoculation (sterile-filtered before injection). At this time, the tumors had a volume of $0.57 \pm 0.18\,cm^3$ (HT-29) and $1.05 \pm 0.29\,cm^3$ (DLD-1). The imaging procedure was the same as described for the healthy mice and the experiments complied with regional standards and regulations and were approved by the local authority in Saxony-Anhalt.

3. Results and discussion

3.1. In vitro cytotoxicity and immunogenicity

As the polymers used in this study have been used in medicine in high doses as plasma volume expanders, they can generally be considered to be biocompatible and safe. To support this, cytotoxicity was assessed by MTT-assay in HepG2 cells after treatment with solutions containing 2 mg/mL or 20 mg/mL polymer. The viability of non-treated cells served as control and was defined to be 100%. No significant decrease of cell viability could be observed after the incubation for 24 and 48 h (Fig. 1, $n = 16$ each).

As lipopolysaccharides from various sources are known to be strong inductors of cytokine production, the polysaccharide polymers were also investigated for the production of pro- and anti-inflammatory cytokines. Human PBMC's were isolated and treated with polymer solutions (2 mg/mL). 6 relevant inflammatory cytokines were analyzed by cytometric bead array flow cytometry after incubation for 4 h or 24 h (Fig. 1). The concentration of inflammatory IL-12p70 and of anti-inflammatory IL-10 was determined to be lower than 10 pg/mL in all samples and controls. The positive control (20 ng/mL LPS) showed a tremendous increase of the other pro-inflammatory cytokines (IL-1β, IL-6, IL-8, and TNF), whereas the concentration in the samples treated with HES 450 (2 mg/mL) was comparable to the non-treated control. The cell supernatants treated with HES 200 and DEX 500 showed a slightly increased cytokine concentration compared to the non-treated control, especially for IL-8, which is an activator of neutrophils and mediator of angiogenesis, but also binds to erythrocytes (Baggiolini & Clark-Lewis, 1992; Koch et al., 1992). However, the concentration of IL-8 in cell supernatants from the LPS treated control was much higher and exceeded the upper detection limit of 23,000 pg/mL. IL-8 was also produced in the negative control ($160\,pg/mL \pm 113\,pg/mL$). In consistency with numerous studies investigating the immunogenicity of hydroxyethyl starches, the polymers used in this study can be regarded as safe and biocompatible (Collis et al., 1994; Lv, Zhou, Zhang, & Xu, 2005; Tian, Lin, Li, & Xu, 2005; Vincent, 2007).

3.2. Synthesis of stable polymer–dye conjugates

All three polymers were conjugated with a fluorescence dye as a preparatory step for the *in vivo* studies by optical imaging (Fig. 2A). A NIR fluorescent probe was chosen for conjugation because of good light penetration in the "optical window", which provides information also from deep tissues (Leblond et al., 2010; Weissleder, 2001). To form a stable and physiologically noncleavable amide bond (Brinkley, 1992), the polymers were amine-modified prior to dye conjugation. Therefore, HES 200 and HES 450 were activated with p-toluenesulfonyl chloride, using a modified method based on a previously described protocol (Besheer et al., 2009). Dextran was activated with p-toluenesulfonyl chloride in water, as the previous method did not work for DEX 500 because of insufficient solubility in DMF. Success of the reactions was monitored by ^{1}H-NMR in D_2O after purification by dialysis and lyophilization (Fig. 2B). The substitution degree with toluenesulfonyl esters was determined to be about 2% per anhydrous glucose unit (AGU) for all polymers by calculation of the peak ratio of the aromatic protons (δ 7.4 and 7.75) to the proton at the alpha-carbon atom (C_1, δ 5–6) of the AGU (Besheer et al., 2009):

$$\mathrm{DS}[\%] = \frac{\mathrm{area}(7.4\,\mathrm{ppm}) + \mathrm{area}(7.75\,\mathrm{ppm})}{4\,\mathrm{protons} \times \mathrm{area}(\mathrm{C1} - \mathrm{proton\ peaks})}.$$

In the following step, the activated polymer was then exposed to 500-fold molar excess of ethylene diamine in a mixture of borax buffer/DMF (pH 9.5) to prevent cross-linking reactions. Reaction success was proven by the disappearance of the signal of aromatic protons in the ^{1}H-NMR spectra after sample purification. The succinimidyl activated fluorescent dye IR800CW (NHS-ester) was conjugated to the amine-modified polymers in bi-distilled water *via* an amide bond. The amount of dye conjugated to the polymers was determined afterwards by fluorescence imaging (Fig. 2C). The conjugation efficiencies were determined to be 90% (HES 200), 80% (HES 450) and 75% (DEX 500).

3.3. Particle size and molecular weight distribution

The particle size and molecular weight distribution were characterized for the three polymers before and after modification. DLS measurements from unmodified polymers indicated a broad distribution of particle sizes (Table 1). The broad molecular weight distribution was confirmed by AF4 measurements (M_W/M_N between 3.6 and 4.4, $n = 3$). AF4 has the advantage that the polymers are separated according to their size before they are detected in the light scattering detector. Therefore monomodal size distributions are measured at each time point during sample elution, which results in precise distribution results. By combining the light scattering signal with the sample concentration, which is obtained from the RI signal, the molecular weight can be calculated (Folta-Stogniew & Williams, 1999). The AF4 results are summarized in Table 2 and also indicate the presence of a fraction with lower molecular weight in all polymers (Fig. 3A–C). Generally, the *z*-average diameters measured by dynamic light scattering ($n = 4$) were smaller than those determined by AF4, but the trend that polymers with higher molecular weight have also a larger particle size was comparable for all polymers. The results show the influence of the syntheses on the molecular weight distribution of the polymers. Competing processes can be discussed as reason: First degradation reactions are likely to occur during the amine-modification (pH ~10). Especially DEX 500, which was reacted at 70 °C, showed a strong decrease of the molecular weight after this step. Second, the polymers can self-aggregate during the reaction which could explain the increased molecular weight of HES 450. Furthermore, using ethylene diamine, cross-linking of molecules might occur, although 500-fold molar excess was used. It was unfortunately not possible to determine the molecular weight distribution of the dye-conjugates by DLS and AF4/MALLS due to interferences of the fluorescent dye with the instrument's laser. However, the NHS-ester of the fluorescent dye cannot lead to cross linking reactions and enhanced self-assembly of the molecules is unlikely due to the hydrophilic and highly negatively charged nature of the dye. Also, the AF4 elution profile was not altered compared to those of the respective amine-modified polymers (RI-detector) and therefore a significant change in the molecular weight distribution is very unlikely. The broad molecular weight distributions of the plasma expanders can generally be regarded as a disadvantage compared to synthetic polymers, which often have more narrow distributions and low polydispersities, given the synthesis is well controlled. On the other hand, polysaccharide based polymers are available at a very large scale inexpensively and still could be further processed or fractionated to obtain polymers with narrow molecular weight

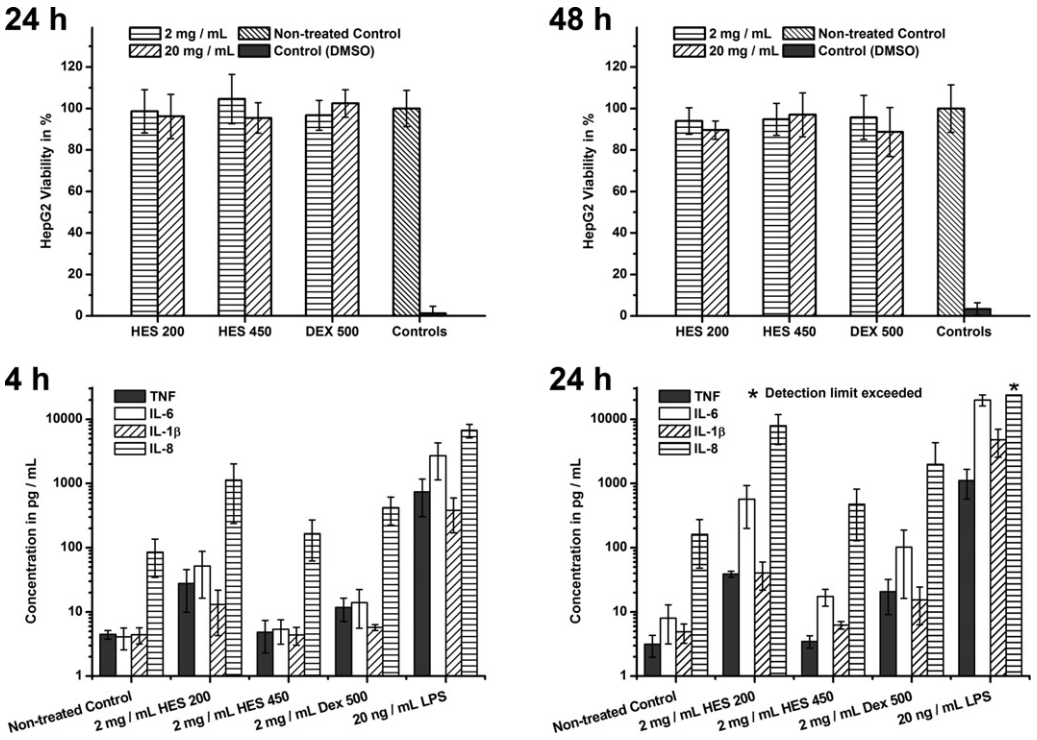

Fig. 1. Top: cell viability of hepatocellular carcinoma cells (HepG2) after incubation with polymer solutions (data represents mean ± SD, $n = 16$). Bottom: cytokine concentration measured in cell supernatants of human PBMC's after incubation with polymer solutions (data represents mean ± SD, $n = 3$).

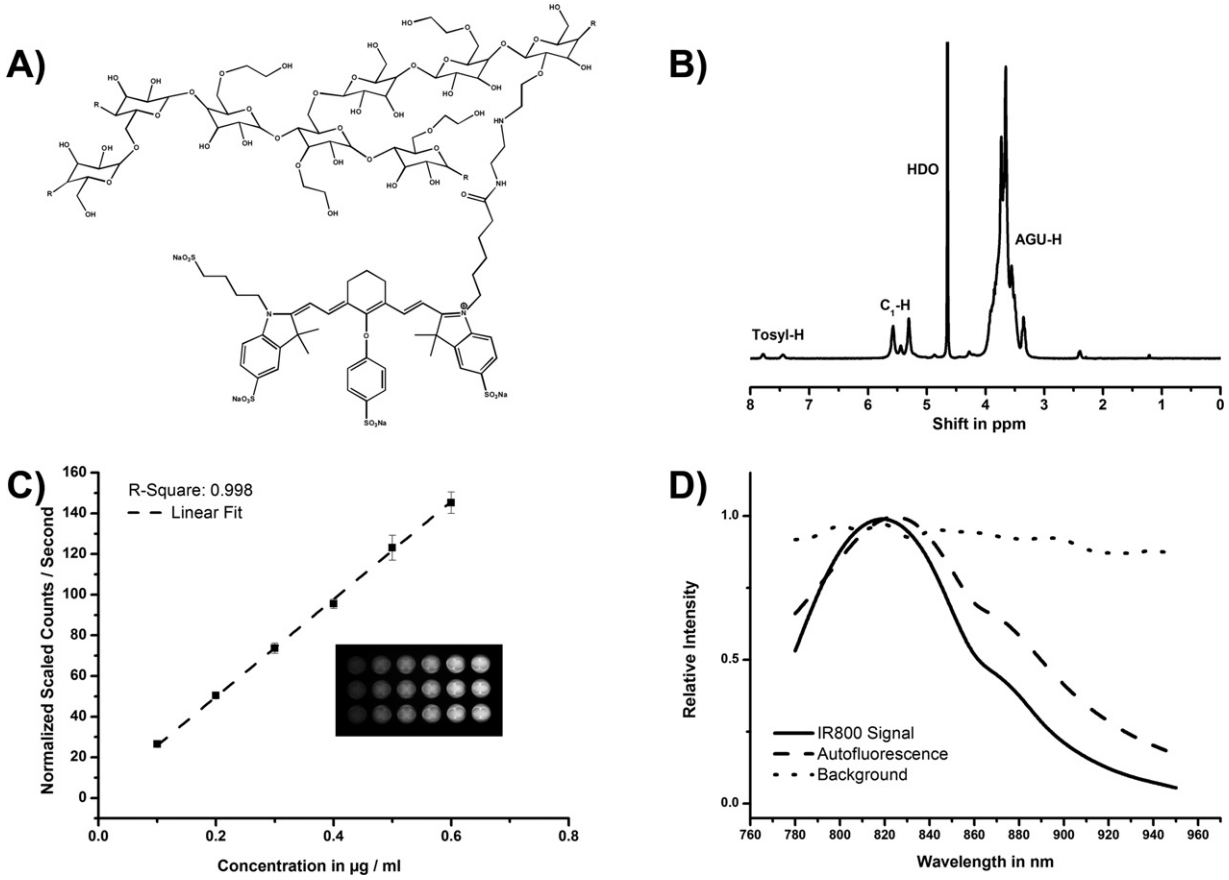

Fig. 2. (A) Representative part of the structure of NIR fluorescent hydroxyethyl starch. (B) Representative NMR spectrum of the tosyl-activated precursor (Tosyl-HES 450). (C) Calibration Curve of the fluorescent dye ($n = 3$), which was used for quantification of conjugation efficiency. (D) Normalized spectra of fluorescence from IR800, autofluorescence and background fluorescence.

Table 1
Particle size and polydispersity of the carbohydrates obtained from DLS. D_Z: *z*-average mean square diameter, $n = 4$.

Polymer	HES 200/0.5	HES 450/0.7	Dextran 500
D_Z	18 nm ± 0.2 nm	24 nm ± 0.4 nm	33 nm ± 0.5 nm
Polydispersity index	0.24 ± 0.01	0.29 ± 0.03	0.41 ± 0.02

Table 2
AF4 results of the polysaccharide-based polymers. D_Z: *z*-average mean square diameter; M_W: weight-average molar mass; M_N: number-average molar mass; M_W/M_N: polydispersity.

Polymer	Unmodified polymers AF4 results			Amine-modified polymers AF4 results			IR800CW
	D_Z (nm)	M_W (kDa)	M_W/M_N	D_Z (nm)	M_W (kDa)	M_W/M_N	Content (%m/m)
HES 200/0.5	26 ± 2	230 ± 5	3.6	33.6 ± 5	128 ± 7	2.0	0.55
HES 450/0.7	36 ± 1	383 ± 18	4.4	49.1 ± 5	623 ± 3	4.8	0.43
Dextran 500	50 ± 5	486 ± 38	3.6	75.5 ± 17	104 ± 10	2.0	0.37

distribution. However, the non-fractionated material was used in our experiments.

3.4. Biodistribution studies

The biodistribution of the conjugated polymers was investigated in nude mice by multispectral optical imaging. Four mice of each group were injected intravenously with 1.5 mg polymer in 100 μL isotonic solution (sorbitol). The background signal and the autofluorescence of the mice were subtracted from the emitted fluorescence by the Maestro® software and the total fluorescence signal was compared to the total initial fluorescence after injection. Dextran accumulated strongly and rapidly in the liver of the mice, whereas the hydroxyethyl starches were distributed much more homogeneously (Fig. 4A). All polymers – and especially dextran – accumulated also in regions of lymph nodes. Investigations of the autopsied organs confirmed the strong liver accumulation of DEX 500, whereas no particular accumulation of both hydroxyethyl starches was found (Fig. 4B). Liver accumulation is undesired as it will lead to increased elimination and liver toxicity (Gaur et al., 2000; Storm, Belliot, Daemen, & Lasic, 1995). It could occur due to receptor mediated uptake into hepatocytes (Nishikawa et al., 1993) and/or RES mediated uptake into the Kupffer cells. The uptake by macrophages and Kupffer cells in liver and spleen is dependent on the structure, size, charge and surface polarity of the particles (Adams, Lavasanifar, & Kwon, 2003; De Jong et al., 2008; Owens & Peppas, 2006). It is clearly an advantage of the hydroxyethyl starches not to accumulate in the liver or spleen, which can be probably attributed to the very hydrophilic surface that prevents the recognition and removal from the blood stream by the reticuloendothelian system. All polymers were detectable in mice for several days, whereas the fluorescence intensity from an ester of dextran 500 with the same dye (control) decreased to 3% of the initial fluorescence intensity within 1 day, probably due to the rapid cleavage of the ester in the blood stream. No liver-accumulation was observed after the injection of the dextran-ester, which leads to the conclusion that the rapid cleavage of the ester happened faster than the liver-accumulation of dextran. All polymers showed

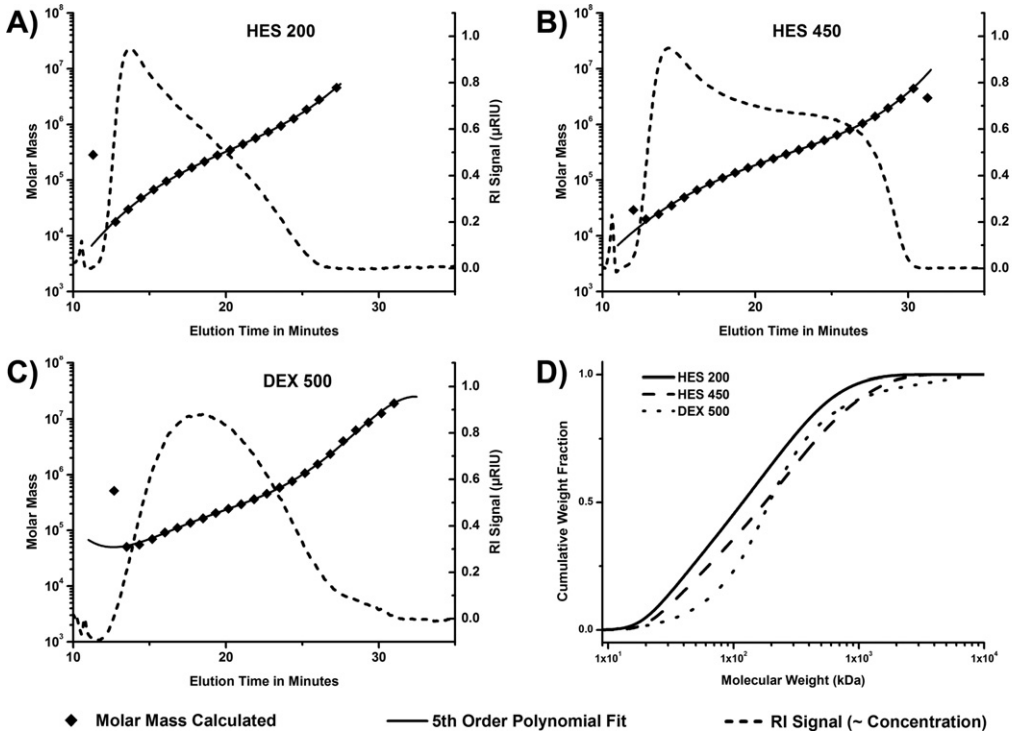

Fig. 3. (A–C) Elution profile of HES 200, HES 450 and DEX 500. The RI signal corresponds with polymer concentration. All polymers showed a broad distribution. (D) Cumulative molecular weight distribution of unmodified HES 200, HES 450 and DEX 500.

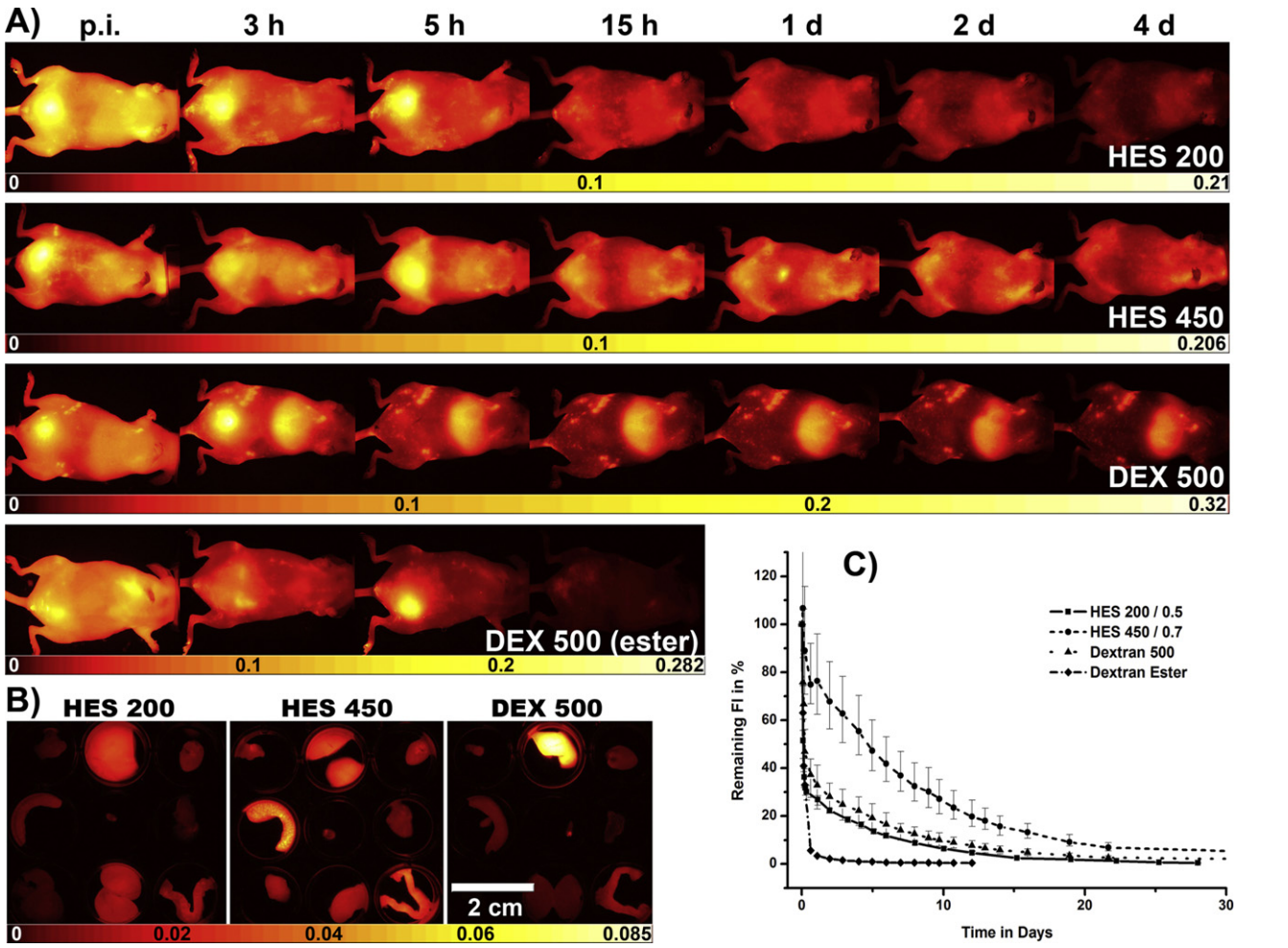

Fig. 4. (A) Representative *in vivo* images after injection of 1.5 mg polymer–NIR conjugate. Bladder signal indicates renal excretion. Strong liver accumulation can be seen for dextran. (B) *Ex vivo* images of the autopsied organs from one mouse of each group 1 day after injection. For each image from left to right–top: fat, liver, heart; middle: spleen, gallbladder, lung; bottom: intestine, kidneys, ovaries. (C) Decrease of fluorescence intensity over several days indicates a slow elimination of the polymers (data represents mean ± min/max, $n = 3$).

a rapid initial decrease of the fluorescence intensity that can be explained by the rather broad molecular weight distribution. The lower molecular weight fraction – below renal excretion threshold – is rapidly excreted with the urine, which is also evident in a strong bladder signal in the first hours after injection (Fig. 4A). We exclude the presence of esters that might have been formed theoretically during the reaction as a side product because amines are much better nucleophiles than hydroxyl-groups. HES 450 was excreted very slowly compared to the other polymers, which can be attributed to the higher molecular weight compared to HES 200 on the one hand and to the higher degree of substitution with hydroxyethyl groups (HES 450:0.7/AGU; HES 200:0.5/AGU) reducing enzymatic degradation on the other hand (Kulicke, Roessner, & Kull, 1993). Especially substitution at C_2 and high substitution degrees are known to slow down enzymatic degradation effectively (Treib et al., 1995). These results are in good agreement with a study in humans (Ferber, Nitsch, & Förster, 1985). The fluorescence intensity from HES 450 did not decrease below 5% of the initial fluorescence intensity up to 22 days after injection (Fig. 4C). The elimination kinetics was not only dependent on the molecular weight distribution, but also on the structure of the polymers. Dextran 500 (D_Z: ≈100 kDa) was slower eliminated than HES 200 (D_Z: ≈130 kDa), which can be explained on the one hand with the increased liver uptake and accumulation and on the other hand with the more branched structure of dextran.

3.5. Tumor accumulation in xenografts

Previous experiments with synthetic HPMA copolymers suggested that EPR-based accumulation of polymers in colon carcinomas is time dependent in the scale of days (Hoffmann et al., 2012). Due to the long circulation time and rather slow initial decrease of the fluorescence intensity, HES 450 was chosen as the most suitable candidate for a possible tumor targeted delivery. Mice were imaged *in vivo* for 42 h and sacrificed afterwards with respect to the tumor burden (Fig. 5A). Apart from a stronger signal at the tumor rim (rim-effect), the distribution of HES 450 in the tumors was rather homogeneous. A rim-effect in both colon carcinoma xenografts was already observed by MRI (Caysa, Metz, Mäder, & Mueller, 2011). It can be explained by various histological differences in the tumor structure compared to the central region (Matsubayashi et al., 2000). No particular difference in tumor accumulation between the two xenograft models was observed, which is in agreement with results obtained with HPMA copolymers (Hoffmann et al., 2012). For better comparability of the fluorescence images, a "tumor accumulation value" (TAV) was calculated, which is a comparable number describing the increased intensity in the tumor compared to that in the remaining mouse body (Hoffmann et al., 2012). Analysing the TAV, the time dependent tumor accumulation of HES 450, which is independent from the tested xenograft model, was confirmed (Fig. 5B). With HES 450, at least a comparable

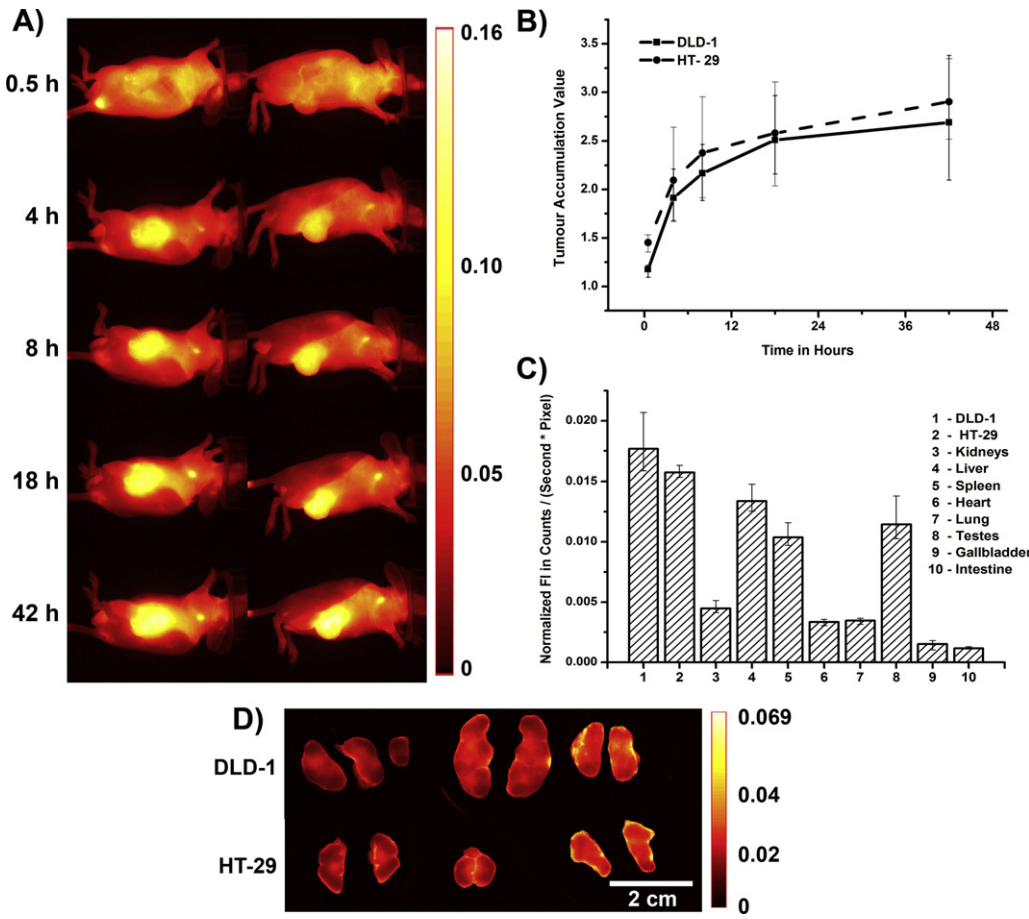

Fig. 5. (A) *In vivo* images of one colon carcinoma xenograft bearing mouse after injection of 1.5 mg HES 450. Left: HT-29, right DLD-1. (B) A comparable tumor accumulation value was calculated from the images for both tumors. (C) The fluorescence intensity measured from organs that were extracted 2 days after injection of HES 450. (D) *Ex vivo* images of autopsied xenograft colon carcinomas from 3 mice 2 days after injection of HES 450.

tumor accumulation as described for 200 kDa HPMA copolymers (DLD-1: 2.02 ± 0.22 and HT-29: 2.05 ± 0.11 after 49 h) was achieved already after 42 h (DLD-1: 2.69 ± 0.65 and HT-29: 2.90 ± 0.42). As the number of animals in this pilot study was small, this result needs further confirmation. All mice were sacrificed 42 hours after injection. The tumors and other organs were autopsied to explore distribution within the tumors (Fig. 5D). Comparing the fluorescence intensity from the tumors with other autopsied mouse organs a specific high local accumulation in the tumors could be confirmed (Fig. 5C). The highest fluorescence intensity was measured in both tumors, followed by liver, spleen and testes. The polymer presence in liver and spleen can be explained by a combination of nonspecific RES-uptake and the comparably high blood content of these organs. A high concentration of ^{14}C-HES (165 kDa) in the testis after intravenous injection into rabbits has already been reported (Yoshida, Amino, & Kishikawa, 1984), but the mechanism has not been investigated so far. The high concentration in the testes could not be observed in our previous biodistribution studies as female mice were used here. However, potential accumulation in testes should be investigated in more detail in further studies.

4. Conclusion

Polysaccharide-based polymers are an interesting alternative to synthetic polymers for polymer therapeutics or diagnostics. They are inexpensive and available in large quantities with a broad range of molecular weights and substitution degrees (Mizrahy & Peer, 2012; Goodarzi et al., 2012). The polymers used in this study are generally accepted as safe for use in humans and have been used in high doses as plasma volume expanders for many years in the clinic. We demonstrated that these polymers are nontoxic to hepatocellular carcinoma cells (HepG2) and have low immunogenic potential, which is consistent with previous literature reports. Further, we showed that it is basically possible to develop polymeric drug delivery systems for tumor targeted drug delivery based on these polymers with varying elimination kinetics. All polymers showed a broad molecular weight distribution, which presents a certain disadvantage compared to synthetic polymers. Amine-modification had a notable effect on the molecular weight distribution, which has to be investigated in more detail in further studies. The highly cross-linked dextran accumulated much more in the liver compared to the hydroxyethyl starches. Moreover, dextran was excreted slower than the larger HES 200 (amine-modified polymers), which could be ascribed to the pronounced liver uptake. For the hydroxyethyl starches, no specific accumulation in liver or spleen was found. This is an advantage over most nanoparticles or nanocapsules, even when they are coated with hydrophilic polymers (Schädlich et al., 2011). Based on the *in vivo* data in healthy mice, the most promising polymer (HES 450) was used to demonstrate the EPR-based passive accumulation in xenograft colon carcinomas. A comparable tumor accumulation was measured as it was recently reported for HPMA copolymers in the same tumor models. Our results emphasize the potential of polysaccharide-based polymers as contrast agent for solid tumor or metastasis detection or possible drug delivery systems for tumor therapy and prove that tumor accumulation is possible using this class of well-known polymers.

Acknowledgements

The authors would like to thank the Deutsche Forschungsgemeinschaft for financial support (MA 1648/7-1; MA 1648/8-1) and the Serumwerk Bernburg AG for the kind provision of the polymers. Further, the Zentrum für Medizinische Grundlagenforschung (ZMG) of the University of Halle Wittenberg is acknowledged for the animal care, especially C. Gottschalk and M. Hennicke. The Core Facility Zellanalyse und Zellsortierung of the university hospital of the MLU Halle-Wittenberg is appreciated for the possibility to use the LSR II Fortessa™. U. Mentzel is acknowledged for her continuous laboratory assistance and S. Kempe, C. Kirbs and S. Drescher are acknowledged for stimulating discussions. E.B. and J.S. are acknowledged for donating their blood for PBMC isolation.

References

Adams, M. L., Lavasanifar, A., & Kwon, G. S. (2003). Amphiphilic block copolymers for drug delivery. *Journal of Pharmaceutical Sciences*, *92*, 1343–1355.

Bae, Y., & Kataoka, K. (2009). Intelligent polymeric micelles from functional poly(ethylene glycol)–poly(amino acid) block copolymers. *Advanced Drug Delivery Reviews*, *61*, 768–784.

Baggiolini, M., & Clark-Lewis, I. (1992). Interleukin-8, a chemotactic and inflammatory cytokine. *FEBS Letters*, *307*, 97–101.

Besheer, A., Hertel, T. C., Kressler, J., Mäder, K., & Pietzsch, M. (2009). Enzymatically catalyzed HES conjugation using microbial transglutaminase: Proof of feasibility. *Journal of Pharmaceutical Sciences*, *98*, 4420–4428.

Bowman, H. W. (1953). Clinical evaluation of dextran as a plasma volume expander. *Journal of the American Medical Association*, *153*, 24–26.

Brinkley, M. (1992). A brief survey of methods for preparing protein conjugates with dyes, haptens and crosslinking reagents. *Bioconjugate Chemistry*, *3*, 2–13.

Caysa, H., Metz, H., Mäder, K., & Mueller, T. (2011). Application of Benchtop-magnetic resonance imaging in a nude mouse tumor model. *Journal of Experimental & Clinical Cancer Research*, 30.

Collis, R. E., Collins, P. W., Gutteridge, C. N., Kaul, A., Newland, A. C., Williams, D. M., et al. (1994). The effect of hydroxyethyl starch and other plasma volume substitutes on endothelial cell activation; an in vitro study. *Intensive Care Medicine*, *20*, 37–41.

De Jong, W. H., Hagens, W. I., Krystek, P., Burger, M. C., Sips, A. J. A. M., & Geertsma, R. E. (2008). Particle size-dependent organ distribution of gold nanoparticles after intravenous administration. *Biomaterials*, *29*, 1912–1919.

Duncan, R. (2009). Development of HPMA copolymer–anticancer conjugates: Clinical experience and lessons learnt. *Advanced Drug Delivery Reviews*, *61*, 1131–1148.

Duncan, R., Ringsdorf, H., & Satchi-Fainaro, R. (2006). Polymer therapeutics: Polymers as drugs, drug and protein conjugates and gene delivery systems: Past, present and future opportunities. *Advances in Polymer Science*, *192*, 1–8.

Euhus, D. M., Hudd, C., Laregina, M. C., & Johnson, F. E. (1986). Tumor measurement in the nude mouse. *Journal of Surgical Oncology*, *31*, 229–234.

Ferber, H. P., Nitsch, E., & Förster, H. (1985). Studies on hydroxyethyl starch. Part II: Changes of the molecular weight distribution for hydroxyethyl starch types 450/0.7, 450/0.5, 450/0.3, 300/0.4, 200/0.7, 200/0.5, 200/0.3 and 200/0.1 after infusion in serum and urine of volunteers. *Arzneimittel-Forschung*, *35*, 615.

Folta-Stogniew, E., & Williams, K. (1999). Determination of molecular masses of proteins in solution: implementation of an HPLC size exclusion chromatography and laser light scattering service in a core laboratory. *Journal of Biomolecular Techniques*, *10*, 51–63.

Garnett, M. C. (2001). Targeted drug conjugates: Principles and progress. *Advanced Drug Delivery Reviews*, *53*, 171–216.

Gaur, U., Sahoo, S. K., De, T. K., Ghosh, P. C., Maitra, A., & Ghosh, P. K. (2000). Biodistribution of fluoresceinated dextran using novel nanoparticles evading reticuloendothelial system. *International Journal of Pharmaceutics*, *202*, 1–10.

Gillies, E. R., & Frechet, J. M. J. (2005). Dendrimers and dendritic polymers in drug delivery. *Drug Discovery Today*, *10*, 35–43.

Goodarzi, N., Varshochian, R., Kamalinia, G., Atyabi, F., & Dinarvand, R. (2012). A review of polysaccharide cytotoxic drug conjugates for cancer therapy. *Carbohydrate Polymers*, *92*, 1280–1293.

Haag, R., & Kratz, F. (2006). Polymer therapeutics: Concepts and applications. *Angewandte Chemie International Edition*, *45*, 1198–1215.

Hey, T., Knoller, H., & Vorstheim, P. (2011). Half-life extension through HESylation. In *Therapeutic proteins: Strategies to modulate their plasma half-lives*. Wiley Online Library.117–140.

Hoffmann, S., Vystrcilová, L., Ulbrich, K., Etrych, T., Caysa, H., Mueller, T., et al. (2012). Dual fluorescent HPMA copolymers for passive tumour targeting with pH-sensitive drug release: Synthesis and characterisation of distribution and tumour accumulation in mice by noninvasive multispectral optical imaging. *Biomacromolecules*, *13*, 652–653.

Koch, A. E., Polverini, P. J., Kunkel, S. L., Harlow, L. A., DiPietro, L. A., Elner, V. M., et al. (1992). Interleukin-8 as a macrophage-derived mediator of angiogenesis. *Science (New York, NY)*, *258*, 1798.

Kopecek, J., & Kopeckova, P. (2010). HPMA copolymers: Origins, early developments, present, and future. *Advanced Drug Delivery Reviews*, *62*, 122–149.

Kulicke, W. M., Kaiser, U., Schwengers, D., & Lemmes, R. (1991). Measurements of the refractive index increment on hydroxyethyl starch as a basis for absolute molecular weight determinations. *Starch*, *43*, 392–396.

Kulicke, W. M., Roessner, D., & Kull, W. (1993). Characterization of hydroxyethyl starch by polymer analysis for use as a plasma volume expander. *Starch*, *45*, 445–450.

Lammers, T., & Ulbrich, K. (2010). HPMA copolymers: 30 years of advances. *Advanced Drug Delivery Reviews*, *62*, 119–121.

Leblond, F., Davis, S. C., Valdes, P. A., & Pogue, B. W. (2010). Pre-clinical whole-body fluorescence imaging: Review of instruments, methods and applications. *Journal of Photochemistry and Photobiology B: Biology*, *98*, 77–94.

Lee, W. H., Jr., Cooper, N., Weidner, M. G., Jr., & Murner, E. S. (1968). Clinical evaluation of a new plasma expander, hydroxyethyl starch. *The Journal of Trauma*, *8*, 381.

Lv, R., Zhou, W., Zhang, L. D., & Xu, J. G. (2005). Effects of hydroxyethyl starch on hepatic production of cytokines and activation of transcription factors in lipopolysaccharide-administered rats. *Acta Anaesthesiologica Scandinavica*, *49*, 635–642.

Maeda, H. (2001). The enhanced permeability and retention (EPR) effect in tumor vasculature: the key role of tumor-selective macromolecular drug targeting. *Advances in Enzyme Regulation*, *41*, 189–207.

Maeda, H., & Matsumura, Y. (2011). EPR effect based drug design and clinical outlook for enhanced cancer chemotherapy. *Advanced Drug Delivery Reviews*, *63*, 129–130.

Matsubayashi, R., Matsuo, Y., Edakuni, G., Satoh, T., Tokunaga, O., & Kudo, S. (2000). Breast masses with peripheral rim enhancement on dynamic contrast-enhanced MR images: Correlation of MR findings with histologic features and expression of growth factors1. *Radiology*, *217*, 841–848.

Matsumura, Y., & Maeda, H. (1986). A new concept for macromolecular therapeutics in cancer chemotherapy: Mechanism of tumoritropic accumulation of proteins and the antitumor agent smancs. *Cancer Research*, *46*, 6387–6392.

Mizrahy, S., & Peer, D. (2012). Polysaccharides as building blocks for nanotherapeutics. *Chemical Society Reviews*, *41*, 2623–2640.

Morita, J., Nakatsuji, H., Misaki, T., & Tanabe, Y. (2005). Water-solvent method for tosylation and mesylation of primary alcohols promoted by KOH and catalytic amines. *Green Chemistry*, *7*, 711–715.

Navickis, R. J., Haynes, G. R., & Wilkes, M. M. (2012). Effect of hydroxyethyl starch on bleeding after cardiopulmonary bypass: A meta-analysis of randomized trials. *Journal of Thoracic and Cardiovascular Surgery*, *144*, 223–230.e5.

Nishikawa, M., Kamijo, A., Fujita, T., Takakura, Y., Sezaki, H., & Hashida, M. (1993). Synthesis and pharmacokinetics of a new liver-specific carrier, glycosylated carboxymethyl-dextran, and its application to drug targeting. *Pharmaceutical Research*, *10*, 1253–1261.

Noga, M., Edinger, D., Rödl, W., Wagner, E., Winter, G., & Besheer, A. (2012). Controlled shielding and deshielding of gene delivery polyplexes using hydroxyethyl starch (HES) and alpha-amylase. *Journal of Controlled Release*, *159*, 92–103.

Owens, D. E., & Peppas, N. A. (2006). Opsonization, biodistribution, and pharmacokinetics of polymeric nanoparticles. *International Journal of Pharmaceutics*, *307*, 93–102.

Perner, A., Haase, N., Guttormsen, A. B., Tenhunen, J., Klemenzson, G., Åneman, A., et al. (2012). Hydroxyethyl starch 130/0.4 versus Ringer's acetate in severe sepsis. *New England Journal of Medicine*, *367*, 124–134.

Schädlich, A., Hoffmann, S., Mueller, T., Caysa, H., Rose, C., Göpferich, A., et al. (2012). Accumulation of nanocarriers in the ovary: A neglected toxicity risk? *Journal of Controlled Release*, *160*, 105–112.

Schädlich, A., Rose, C., Kuntsche, J., Caysa, H., Mueller, T., Göpferich, A., et al. (2011). How stealthy are PEG-PLA nanoparticles? An NIR in vivo study combined with detailed size measurements. *Pharmaceutical Research*, *28*, 1995–2007.

Storm, G., Belliot, S. O., Daemen, T., & Lasic, D. D. (1995). Surface modification of nanoparticles to oppose uptake by the mononuclear phagocyte system. *Advanced Drug Delivery Reviews*, *17*, 31–48.

Tian, J., Lin, X., Li, Y. H., & Xu, J. G. (2005). Influence of hydroxyethyl starch on lipopolysaccharide-induced tissue nuclear factor kappa B activation and systemic TNF-γ expression. *Acta Anaesthesiologica Scandinavica*, *49*, 1311–1317.

Tomayko, M. M., & Reynolds, C. P. (1989). Determination of subcutaneous tumor size in athymic (nude) mice. *Cancer Chemotherapy and Pharmacology*, *24*, 148–154.

Treib, J., Haass, A., Pindur, G., Seyfert, U. T., Treib, W., Grauer, M. T., et al. (1995). HES 200/0.5 is not HES 200/0.5. Influence of the C2/C6 hydroxyethylation ratio of hydroxyethyl starch (HES) on hemorheology, coagulation and elimination kinetics. *Thrombosis and Haemostasis*, *74*, 1452–1456.

Ulbrich, K., Subr, V., Strohalm, J., Plocova, D., Jelinkova, M., & Rihova, B. (2000). Polymeric drugs based on conjugates of synthetic and natural macromolecules: I. Synthesis and physico-chemical characterisation. *Journal of Controlled Release*, *64*, 63–79.

Vicent, M. J., Ringsdorf, H., & Duncan, R. (2009). Polymer therapeutics: Clinical applications and challenges for development. *Advanced Drug Delivery Reviews*, *61*, 1117–1120.

Vincent, J. L. (2007). The pros and cons of hydroxyethyl starch solutions. *Anesthesia & Analgesia*, *104*, 484–486.

Weissleder, R. (2001). A clearer vision for in vivo imaging. *Nature Biotechnology*, *19*, 316–317.

Wöhl-Bruhn, S., Badar, M., Bertz, A., Tiersch, B., Koetz, J., Menzel, H., et al. (2012). Comparison of in vitro and in vivo protein release from hydrogel systems. *Journal of Controlled Release*, *162*, 127–133.

Wöhl-Bruhn, S., Bertz, A., Harling, S., Menzel, H., & Bunjes, H. (2012). Hydroxyethylstarch-based polymers for the controlled release of biomacromolecules from hydrogel microspheres. *European Journal of Pharmaceutics and Biopharmaceutics*, *81*, 573–581.

Yoshida, M., Amino, M., & Kishikawa, T. (1984). A study of hydroxyethyl starch. Long pursuit of hydroxyethyl starch after consecutive infusions into rabbits. *Starch*, *36*, 240–246.